Submitted to Physical Review

RECEIVED
LAWRENCE
RADIATION LABORATORY

UCRL-20635
Preprint

c 2

DOCUMENTS SECTION

S-CHANNEL DOMINANCE AND CHARGE RATIOS IN HIGH-ENERGY PION PHOTOPRODUCTION

I. Barbour, W. Malone, and R. G. Moorhouse

March 18, 1971

AEC Contract No. W-7405-eng-48

TWO-WEEK LOAN COPY

This is a Library Circulating Copy which may be borrowed for two weeks. For a personal retention copy, call Tech. Info. Division, Ext. 5545

LAWRENCE RADIATION LABORATORY
UNIVERSITY of CALIFORNIA BERKELEY

UCRL-20635 c.2

34a

DISCLAIMER

This document was prepared as an account of work sponsored by the United States Government. While this document is believed to contain correct information, neither the United States Government nor any agency thereof, nor the Regents of the University of California, nor any of their employees, makes any warranty, express or implied, or assumes any legal responsibility for the accuracy, completeness, or usefulness of any information, apparatus, product, or process disclosed, or represents that its use would not infringe privately owned rights. Reference herein to any specific commercial product, process, or service by its trade name, trademark, manufacturer, or otherwise, does not necessarily constitute or imply its endorsement, recommendation, or favoring by the United States Government or any agency thereof, or the Regents of the University of California. The views and opinions of authors expressed herein do not necessarily state or reflect those of the United States Government or any agency thereof or the Regents of the University of California.

S-CHANNEL DOMINANCE AND CHARGE RATIOS IN HIGH-ENERGY PION PHOTOPRODUCTION*

I. Barbour and W. Malone

Department of Natural Philosophy
Glasgow University, Glasgow, Scotland

and

R. G. Moorhouse

Department of Physics and Lawrence Radiation Laboratory
University of California, Berkeley, California 94720

March 18, 1971

ABSTRACT

It is shown that an explicit quark model, or duality diagrams, imply certain charge ratios on the square of the imaginary parts of amplitudes for $\gamma N \to \pi^{\pm} N$ and $\gamma N \to \pi^{\pm} \Delta$, which are experimentally observed to hold on the high energy cross sections $\frac{d\sigma}{dt}$ for $-0.2 \geq t \geq -0.8$. A fixed-t dispersion relation calculation, using knowledge of the low-energy photoproduction amplitudes, suggests that this may be due to cancellation of the contribution of the low and medium energy s- and u-channel resonances to the real parts of the amplitudes, so that the s-channel dominates the dispersion integral and the quark model relations also apply to the real parts of the amplitudes. In the extreme forward direction $[(-t)^{\frac{1}{2}} \lesssim 0.2]$ the fixed-t dispersion relations indicate

* This work was supported in part by the U.S. Atomic Energy Commission.

that the $\gamma N \rightarrow \pi^{\pm} N$ amplitudes are predominantly real and dominated by the contributions to the dispersion relations of the Born approximation and other very low-energy resonances. Some possible implications for purely hadronic reactions are discussed.

1. INTRODUCTION

It is well known that the differential cross-section for $\gamma p \to \pi^+ n$ exhibits a forward spike in the region $0 > t \geq m_\pi^2$ and that a similar forward spike is given by the gauge invariant pion pole (electric Born approximation). Indeed either the electric Born approximation or the full Born approximation[1] gives fair agreement with the data,[2] both for unpolarized and polarized photons[3] in the spike region, except perhaps for the most forward points measured, as discussed below.

Likewise the differential cross-section for $\gamma n \to \pi^- p$ for $0 > t \geq -m_\pi^2$ is found to be equal[4] to that for π^+ photoproduction and thus also to be given approximately by the Born approximation. But for $-m_\pi^2 > t$ the Born approximation fails badly both for π^+ and π^- photoproduction; in particular one of the most marked features of the data at high energy is that π^- photoproduction is less than π^+ photoproduction away from the forward spike region. For $-0.2 > t > -0.8$

$$\frac{d\sigma}{dt}(\gamma p \to \pi^- p) \Big/ \frac{d\sigma}{dt}(\gamma p \to \pi^+ n) \simeq 0.35. \tag{1}$$

Rather similar though more complicated features exist in the high energy differential cross-sections of the four reactions $\gamma N \to \pi^\pm \Delta$. It has been shown that for $0 > t > -m_\pi^2$ the differential cross sections are given, within their rather large errors, by a gauge invariant pion pole theory[5] (in this case the minimal part of the Born approximation that both contains the pion pole and is gauge invariant). For $0 > t > -m_\pi^2$ the experiments are compatible with

$$\frac{d\sigma}{dt}(\gamma p \to \pi^- \Delta^{++}) = \frac{d\sigma}{dt}(\gamma n \to \pi^+ \Delta^-) \text{ and } \frac{d\sigma}{dt}(\gamma p \to \pi^+ \Delta^0) = \frac{d\sigma}{dt}(\gamma n \to \pi^- \Delta^+),$$

in accord with a gauge invariant pion pole theory.[5] However, away from the extreme forward direction these cross-sections take on remarkably different ratios, as shown in Fig. 1. In the same region of t for which the ratio (1) holds, namely $-0.2 > t > -0.8$ the $\pi^{\pm}\Delta$ photoproduction cross-sections take the following rather constant ratios

$$\frac{d\sigma}{dt}(\gamma n \to \pi^- \Delta^+) \Big/ \frac{d\sigma}{dt}(\gamma p \to \pi^+ \Delta^0) \simeq 0.3 \tag{2a}$$

$$\frac{d\sigma}{dt}(\gamma p \to \pi^- \Delta^{++}) \Big/ \frac{d\sigma}{dt}(\gamma n \to \pi^+ \Delta^-) \simeq 0.5 \tag{2b}$$

$$\frac{d\sigma}{dt}(\gamma p \to \pi^- \Delta^{++}) \Big/ \frac{d\sigma}{dt}(\gamma p \to \pi^+ \Delta^0) \simeq 1.0. \tag{2c}$$

It seems that the high energy experiments on the forward photoproduction of charged pions exhibit three regions of t where the data has definite and distinct characteristics, though in all three regions $(s - M^2)^2 \frac{d\sigma}{dt}$ is approximately constant as a function of s.

(i) $0 > t > -m_\pi^2$. In this region the amplitudes are strongly affected by the exchange of the gauge invariant pion pole (the energy dependence of this Born approximation agreeing with the observed energy dependence). The $\pi^+ n$ and $\pi^- p$ photoproduction cross-sections are equal.

(ii) $-0.2 \geq t \geq -0.8$. The charge ratios for $\pi^{\pm} n$ and $\pi^{\pm}\Delta$ photoproduction are given by (1) and (2) throughout the region. In $\pi^{\pm}\Delta$ photoproduction the logarithmic slopes of $d\sigma/dt$ are constant to within the errors and approximately equal to $e^{2.5t}$; for $\pi^+ n$ the slope

is approximately $e^{1.6t}$.[4] Denote the cross-sections corresponding to photons polarized perpendicular and parallel to the production plane by $\sigma_\perp$ and $\sigma_{||}$ respectively, then by Stichels theorem $\sigma_\perp$ and $\sigma_{||}$ correspond to natural and unnatural parity t-channel exchange respectively. In $\gamma p \to \pi^+ n$, $\sigma_\perp$ is strongly dominant while in $\gamma n \to \pi^- p$, $\sigma_\perp = \sigma_{||}$.

(iii)[4] $-0.8 > t > (?)$. In this region the charge ratios change and the slopes of the differential cross-sections become steeper, the $\pi^\pm\Delta$ slope being about $e^{3.2t}$ and the $\pi^+ n$ slope about $e^{3.8t}$.

It appears that the extreme forward region, (i) above, is partly understood in terms of the Born approximation or a similar theory, and we shall have some comment on that situation. It is the main object of this paper to contribute to the understanding of the region (ii), $-0.2 \geq t \geq -0.8$, and in particular the charge ratios (1) and (2).

Firstly it is rather clear that no simple Regge <u>pole</u> picture can satisfy the data in region (ii). The obviously dominant candidates for natural parity exchange (measured by $\sigma_\perp$) are the exchange degenerate ρ and A_2 trajectories contributing $\beta_\rho(t)(1 - e^{-i\pi\alpha(t)})/\sin \pi\alpha(t) + \beta_A(t)(1 + e^{-i\pi\alpha(t)})/\sin \pi\alpha(t)$ to the amplitudes, with $\alpha(t) = 0$ at $t \simeq -0.6$. <u>Strong</u> exchange degeneracy with $\beta_A = \beta_\rho$ would give a dip in $\sigma_\perp(\gamma p \to \pi^+ n)$ from the necessity that $\beta_A = 0$ at $t \simeq 0.6$; such a dip is conspicuously absent. Weak exchange degeneracy $\beta_A \neq \beta_\rho$ could perhaps avoid the dip, but would lead to a purely real A_2 exchange amplitude (isovector photon) and a purely imaginary ρ exchange amplitude (isoscalar photon) at $t = -0.6$. Since the difference between $\gamma p \to \pi^+ n$ and $\gamma n \to \pi^- p$ photoproduction comes from the isoscalar photon-isovector photon interference term, this implies $\sigma_\perp(\gamma p \to \pi^+ n)$ would

equal $\sigma_{\perp}(\gamma n \to \pi^- p)$ at $t \simeq -0.6$, contrary to an observed ratio of about 4 to 1. Thus it is evident that an explanation in terms of Regge theory requires cuts. For example using the strong absorption model, and varying 28 parameters, Kane et al.[6] obtain a fit to $\gamma p \to \pi^+ n$, $\gamma n \to \pi^- p$ (and $\gamma p \to \pi^0 p$, $\gamma p \to np$ and $\bar{p}p \to \bar{n}n$, $np \to pn$).

We attempt a unified view of the charge ratios (1) and (2a), (2b), (2c) firstly by considering the nucleon, and the Δ, as mainly composed of three quarks and by considering the process of photoproduction as one in which the nucleon is first photoexcited and then de-excited by pion emission. The basic quark diagram is shown in Fig. 2a; the photon excites virtual intermediate states of the quark which decay by pion emission; if the quark is spatially excited, and does not de-excite by interaction with the other two quarks in the diagram, the sum over intermediate states points out the excited quark as the one which emits the pion leading to a quark impulse approximation.

In calculating the ratios (1), (2a), (2b), (2c) in the foregoing quark model the spin and isospin sums over the intermediate quark states are replaced by the unit operator and, apart from the spatial factors, one is left with matrix elements of the form

$$\sum_{i=1}^{3} (N|H^i(\gamma)\, H^i(\pi)|N); \quad \sum_{i=1}^{3} (N|H^i(\gamma)\, H^i(\pi)|\Delta) \; . \qquad (3)$$

In (3) $|N)$ and $|\Delta)$ are SU6 wave functions of the $\{56\}$ representation for the nucleon and Δ respectively; $H^i(\gamma)$ and $H^i(\pi)$ are the interaction Hamiltonians of the ith quark with the photon and pion rexpectively. The isospin sub-operator part of $H^i(\gamma)\, H^i(\pi)$ is, with

the usual electromagnetic couplings of the quarks, proportional to

$$\begin{pmatrix} 2/3 & 0 \\ 0 & -1/3 \end{pmatrix}_i \underline{\tau}^{(i)} \cdot \underline{\pi} \tag{4}$$

In evaluating the ratios (1) and (2) in our model, the spin and spatial matrix elements cancel, whatever the particular form assumed for the interaction. The operator (4) gives rise to the following ratios

$$\frac{d\sigma}{dt}(\gamma n \to \pi^- p) \Big/ \frac{d\sigma}{dt}(\gamma p \to \pi^+ n) = 1/4 \tag{5}$$

$$\frac{d\sigma}{dt}(\gamma n \to \pi^- \Delta^+) \Big/ \frac{d\sigma}{dt}(\gamma p \to \pi^+ \Delta^0) = 1/4 \tag{6a}$$

$$\frac{d\sigma}{dt}(\gamma p \to \pi^- \Delta^{++}) \Big/ \frac{d\sigma}{dt}(\gamma n \to \pi^+ \Delta^-) = 1/4 \tag{6b}$$

$$\frac{d\sigma}{dt}(\gamma p \to \pi^- \Delta^{++}) \Big/ \frac{d\sigma}{dt}(\gamma p \to \pi^+ \Delta^0) = 3/4. \tag{6c}$$

The values (5), (6a), (6b) are, in the context of the model, an immediate consequence of the fact that a π^+ can only be emitted from a proton quark [involving the matrix element 2/3 in (4)] and a π^- can only be emitted from a neutron quark [involving the factor -1/3 in (4)]. In the region $-0.2 \geq t \geq -0.8$ the experimental values (1), (2a), (2b), (2c) are to be compared with (5), (6a), (6b), (6c) respectively. We note an almost quantitative agreement and we notice (as displayed for example in Fig. 1) the remarkable change from the experimental ratios in the pion pole region $(0 > t > -m_\pi^2)$.

An important question in this picture is the possible contribution of the crossed graphs, Fig. 2b, which has been ignored. It is immediately seen that these give contributions whose charge ratios are the inverse of (5), (6a), and (6b) so that a large contribution from the crossed graphs would invalidate our ratios. The uncrossed graphs, (Fig. 2a) giving the ratios correspond to the contributions of s-channel resonances and the crossed graphs (Fig. 2b) to the contributions of u-channel resonances. The u-channel resonances are distant from the forward direction so one expects their contribution to the imaginary part of the amplitudes to be small but distant u-channel and distant s-channel resonances might dominate the real part. This is evidently happening for the particular case where the resonance is the nucleon itself at $t = 0$ where the Born approximation is big and leads to equal amplitudes for $\gamma p \to \pi^+ n$ and $\gamma n \to \pi^- p$, as observed.

One may put these questions in terms of the usual duality picture. If one assumes vector dominance, so that the isoscalar photon is represented by an ω meson and the isovector photon by a ρ^0 meson then the selection rules implied by the duality diagrams will give relations between the <u>imaginary parts</u> of various photoproduction amplitudes.[7] Among these relations for the <u>imaginary parts</u> are our ratios for $\gamma N \to \pi^\pm N$ and $\gamma N \to \pi^\pm \Delta$. (This is immediate on looking at Fig. 2c, which pictures a photon turning into a vector meson, followed by a duality diagram for a vector meson scattering from a baryon into a pion. This figure is just a stretched string version of Fig. 2a, but not of course 2b.) The figure also illustrates that in these relations the full vector dominance assumptions are <u>not</u> being used, but only the

relations between photon coupling to isoscalar and isovector mesons which follow from the photon being a U-spin scalar member of an octet. Such relations seem likely to endure strong modifications of the vector dominance hypothesis, such as the addition of further vector mesons through which the photon interacts with hadronic matter. These duality relations are not ensured for the real parts, just for the same reasons as mentioned above, namely the possibility of large u-channel contributions to the real parts.

Nevertheless the charge ratios indicate that the u-channel contribution is suppressed and we will seek verification and elucidation of this point by investigating, as explicitly as possible, the relative importance of the s- and u-channel contributions to the real part of the high-energy amplitude. The most direct way to do this is through fixed-t dispersion relations and the results of such an investigation are reported in the next section.

2. s- AND u-CHANNEL CONTRIBUTIONS TO THE HIGH ENERGY REAL PARTS OF AMPLITUDES

We wish to consider the relative contributions of the s and u channels to the real parts of the high-energy photoproduction amplitudes, and the most direct way of doing this is through the fixed-t dispersion relations. Because of the lack of detailed low-energy data on $\gamma N \to \pi^{\pm}\Delta$ we will have to confine most of the discussion in this section to $\gamma N \to \pi^{\pm}N$. For either of these processes there are four invariant amplitudes which we will denote by $A_{i+}(s,t)$ for $\gamma p \to \pi^{+}n$ and by $A_{i-}(s,t)$ for $\gamma n \to \pi^{-}p$ where $i = 1,2,3,4$. The fixed-t dispersion relations are[8]

$$\mathrm{Re}\, A_{i\pm}(s,t) = B_{i\pm}(s,u) + \int_{(M+m)^2}^{\infty} ds' \times \left[\frac{\mathrm{Im}\, A_{i\pm}(s',t)}{s'-s} + \xi_i \frac{\mathrm{Im}\, A_{i\mp}(s',t)}{s'-u}\right] \tag{7a}$$

where the Born terms are given by

$$B_{1+}(s,u) = (2)^{\frac{1}{2}} \frac{ge}{4\pi} \frac{1}{s-M^2}, \quad B_{2+}(s,u) = -(2)^{\frac{1}{2}} \frac{ge}{4\pi} \frac{1}{(s-M^2)(t-m^2)}$$

$$B_{3+}(s,u) = -(2)^{\frac{1}{2}} \frac{ge}{4\pi 2M}\left(\frac{\mu_P'}{s-M^2} - \frac{\mu_N'}{u-M^2}\right)$$

$$B_{4+}(s,u) = -(2)^{\frac{1}{2}} \frac{ge}{4\pi 2M}\left(\frac{\mu_P'}{s-M^2} + \frac{\mu_N'}{u-M^2}\right)$$

$$B_{i-}(s,u) = \xi_i\, B_{i+}(u,s)\,. \tag{7b}$$

In (7a) and (7b) $\xi_i = +1$ if $i = 1,2,4$ and $\xi_3 = -1$, M is the nucleon and m the pion mass. The first integral is over the s-channel cut and the second integral comes from the u-channel cut. The cut structure is shown in Fig. 4. In a quark, or duality diagram, picture the amplitude ratios 1/2, $(3/4)^{\frac{1}{2}}$ leading to the ratios (5), (6a), (6b), and (6c) will hold between the appropriate Im A(s',t) on the s-channel cut, as shown in the introduction. However, the $\frac{1}{2}$ ratios will <u>not</u> hold for the Im A or the u-channel cut, which corresponds to u-channel resonances, as in Fig. 2b, rather than s-channel resonances, as in Fig. 2a. For high-energy photoproduction though the u-channel cut is distant from the physical s, we certainly cannot say a priori that the s-channel cut will dominate the right-hand side of Eq. (7). In pion photoproduction itself near $t = 0$ we already know that the s- and u-channel Born poles, which are near together and both very distant from the physical s, are both very important in Re A(s,t) implying an equal importance of an "s-wave" and a "u-cut" contribution. Near $t = 0$ then, all is consistent with a totally real amplitude, into which the Born terms and perhaps a few other low-energy particles or resonances notably the Δ, contribute most importantly from the right-hand side of (7). Since the difference between the energy denominators in the dispersion relations is negligible for integration over low-energy particles or resonances such as the N and Δ, it follows from the crossing symmetry between the A_+ and A_- amplitudes displayed in (7) that the amplitudes for $\gamma p \to \pi^+ n$ and $\gamma n \to \pi^- p$ would then be equal, as is indeed observed.

In the region of somewhat larger values of $-t$, $-0.2 \geq t \geq -0.8$, the cross-sections take on the characteristic ratios (1) and (2), and we know from recoil proton polarization measurements that, at least for $\gamma p \to \pi^+ n$, the amplitudes have an imaginary part. There is no problem with the charge ratios for the imaginary part but we are left with the problem of the real part and there is no evidence that it is small, either from the polarization measurements, or from asymptotic energy dependence considerations discussed in the next section. (If it <u>were</u> small then the smallness would have to be explained by a cancellation similar to that we are about to expound.) In this section we examine the hypothesis that the combined contribution of the s- and u-channel <u>low</u> and <u>medium</u> energy imaginary parts (to the fixed-t dispersion relations giving the high-energy real part) is negligibly small. We use the term low and medium energy relative to the physical energy and for an s value of about 30 the low- and medium-energy cuts might extend up to $s(u) \sim 5\text{-}15$. If this be so it leaves the greater part of $\mathrm{Re}\, A(s,t)$ free to come from the right-hand part of the s cut, say from $s' \gtrsim s/2$, just from the smallness of the energy denominators on the right part of the s-channel cut compared with the large ones from the left-hand part of the u-channel cut. Such a dominance of <u>s-channel</u> imaginary parts in the dispersion relation secures the charge ratios also in the real parts of the amplitudes.

To sustain our hypothesis we have to investigate whether integration over the low- and medium-energy region is likely to give a negligibly small contribution to $\mathrm{Re}\, A(s,t)$. The result is shown in Fig. 5 where we have plotted the contribution to $(s - M^2)^2\, d\sigma/dt$

arising from the real parts only of the amplitudes, evaluated from the dispersion relations (7). The evaluation is done for an incident laboratory momentum of 16 GeV/c [$s \approx 30$ $(\mathrm{GeV/c})^2$], and the photoproduction helicity amplitudes used are those of Walker.[9] We discuss the results in the region $-0.2 \geq t \geq -0.8$.

The highest curve shown is that obtained by taking only the Born terms on the right-hand side of Eqs. (7a) and (7b) and in our t region the result is clearly impossible. If we add to the Born terms the effect of the $\Delta(1236)$ in both the s and u parts of the dispersion integral (7) we get a dramatic drop to the next highest curve, as shown. This effect was already noted by Engels, Schwiderski, and Schmidt[10] in connection with photoproduction at energies between 1 and 3 GeV/c. Next adding to the dispersion relations the $p_{11}(1470)$ and the $s_{11}(1560)$ again leads to a decrease, while there is a further dramatic drop on adding the $d_{13}(1520)$. We should note that at this stage the curve has already dropped to the level of the proton data for $-0.2 > t > -0.5$, and to or below the level of the lowest neutron data for $-0.5 > t > -0.8$. Adding in the third resonance region contribution to the dispersion relations leads to a further drop, but takes us to the end of the helicity amplitude analysis of Walker. There is one more thing we can do in our examination of trends. The $f_{37}(1920)$ is a prominent Δ resonance, the first-Regge recurrence of the $p_{33}(1236)$. If we assume that like the p_{33}, the $f_{37}(1920)$ has only magnetic coupling (as suggested for example by the quark model) and that the coupling is of the same sign as the p_{33} and we take the magnitude of the coupling from

backward π^0 photoproduction[11] then we get the bottom curve (over most of our t region) shown in Fig. 5. (In Walker's fit to the $\pi^{\pm}$ low-energy data nearly all the imaginary part is due to the resonances; the dots represent the final result when the non-resonant background at all energies is also taken into the dispersion integral.) The curves apply with negligible error to either π^+ or π^- photoproduction, as is evident from the crossing symmetry in Eq. (7), since the variation of the energy denominators in the low-energy resonance region is small for large s.

The trend is obvious: as successively higher mass resonances are added to both the s- and u-channel integrals in the fixed-t dispersion relations, the calculated real amplitudes get successively smaller, with the exception of the addition of $p_{11}(1470)$ which has a small influence in the opposite direction. In the interval $-0.5 > t > -0.8$ the result is already of the order of or smaller than the neutron data. The results are shown in another way in Fig. 6, where at the fixed value of $t = -0.4$ we plot the same quantity as in Fig. 5 as a function of the upper limit of integration in the dispersion integrals. It is also obvious that the trend could continue since, though the partial widths higher mass resonances are smaller, the residual amplitudes which they have to cancel are also smaller. We do not attach too much importance to the exact numbers obtained through the dispersion relations since, as pointed out by Walker[9] and by others,[12] the results of the helicity amplitude analysis in the present state of the data are subject to quite large errors.[13-15] We rather point to the

trend which if continued will lead to the mutual cancellation of the low- and medium-energy resonances in the dispersion relations, and thus to satisfactory agreement with the charge ratios for $\gamma p \to \pi^+ n$, $\gamma n \to \pi^- p$.

We may contrast this uni-directional effect of the resonances in the fixed-t dispersion relations in the region $-0.2 > t > -0.8$ to the varied effects in the extreme forward region. We plot the same quantities as before in Fig. 7, but now on the expanded horizontal scale of $(-t)^{\frac{1}{2}}$ appropriate to the extreme forward direction. The experimental points shown are $(s - M^2)^2 \frac{d\sigma}{dt}$ for $\gamma p \to \pi^+ n$, and the evidence is that the $\gamma n \to \pi^- p$ has an equal cross-section for $(-t)^{\frac{1}{2}} < 0.2$. As before the curves are the contribution to $(s - M^2)^2 \frac{d\sigma}{dt}$ of the real parts of the amplitudes calculated from the fixed-t dispersion relations (7), for various resonances included in the integrals. We see that the "Born +Δ" curve is significantly different from the "Born" curve but that the additional effect of adding all other "known" resonances is quite small, so that the final curve remains near "Born +Δ." It is worth noting that one of the forward experimental points is considerably higher than "Born only" and agree more nearly with "Born +Δ" and the other curves clustered around it. In view of the qualitative agreement of the experimental points and the curve, in the extreme forward direction all is compatible with (i) totally real amplitudes, (ii) saturation of the fixed-t dispersion relations by low-energy resonances, including the Born terms. Similar conclusions on the extreme forward region have been reached by previous authors.[1] Our only new addition to their remarks

is that the way the various resonances are contributing makes saturation seem likely, and that this may take place near the Born $+\Delta$ curve, at any rate for $(-t)^{\frac{1}{2}} \lesssim 0.05$.

In view of the importance of s-channel helicity in absorption models,[6] or other models[16] which view the nucleon as a spatially structured scattering object, it is interesting to set out the role of the various s-channel helicity amplitudes in the curves of Figs. 5, 6, and 7. To do this we introduce a nmemonic notation for the helicity amplitudes. For $\gamma N \to \pi N$ there are four independent helicity amplitudes and we take these to be the amplitudes for which the photon has helicity +1; in that case the initial helicities are 3/2 or 1/2 and the final one 1/2 or -1/2. We name the helicity amplitudes corresponding to the various transitions as follows

$$\frac{1}{2} \to \frac{1}{2} : H_0$$

$$\frac{3}{2} \to \frac{1}{2} : H_1$$

$$\frac{1}{2} \to -\frac{1}{2} : H_{-1}$$

$$\frac{3}{2} \to -\frac{1}{2} : H_2 \qquad (8)$$

where suffixes 0, ± 1, and 2 represent no helicity flip, single helicity flip and double helicity flip respectively. We define the normalization and units of our helicity amplitudes to be the same as those of the helicity amplitudes H_1, H_2. H_3, H_4 of Eq. (21) of Walker[9] so that

$$(H_0, H_1, H_{-1}, H_2) \equiv (H_2, H_1, H_4, H_3) \tag{9}$$

and

$$(s - M^2)^2 \frac{d\sigma}{dt} = 2\pi s\{|H_0|^2 + |H_1|^2 + |H_{-1}|^2 + |H_2|^2\}. \tag{10}$$

We now describe the relative magnitudes of the various Re H as evaluated from the dispersion relations (7). In the forward spike Re H_0 is strongly dominant being at $t = -0.0002$ $[(-t)^{\frac{1}{2}} = 0.045]$ more than ten times greater than any other amplitude. This of course is to be expected since the other, spin-flip, amplitudes must vanish at $\theta = 0$; in the language of Harari[16] H_0 is a "J_0" amplitude. Just outside the forward spike at $t = -0.02[(-t)^{\frac{1}{2}} \sim m_\pi]$ Re H_0 is still the largest amplitude, but only 40% larger than Re H_2; both Re H_1 and Re H_γ are more than ten times smaller. At these two t values and in the spike region generally there is only a few percent difference between Re H_0 evaluated using Born +Δ only and evaluated using all the "known" amplitudes (and the same holds for Re H_2).

The situation is very different in region of principal interest $-0.2 \geq t \geq -0.8$. Here for Born +Δ only Re H_2 is largest, Re H_0 is about 30% of Re H_2, and Re H_1 and Re H_{-1} are very small. When the full "known" amplitudes are taken in the dispersion relations both Re H_0 and Re H_2 become considerably smaller (accounting for the drop in the curves of Fig. 5) while Re H_1 becomes non-negligible over a small range around $t = -0.3$ (Re H_1 is a "J_1" amplitude and zeros at around $t = -0.75$).

3. CONNECTION WITH FESR

In the definition of the finite-energy or continuous-moment sum rules, it is implied that the connection between low and high energies is established through the assumption of some asymptotic or high-energy form, for which Regge poles are commonly used. Using the assumption that all the relevant Regge trajectories have small α, which if correct makes their result independent of any particular high-energy Regge model, Jackson and Quigg[17] find a form for the real part of their high-energy amplitude in terms of an integral over the low-energy amplitude. The result is the same as if one were to evaluate the fixed-t dispersion relation (7), neglecting the variation with s' of the energy denominators; this is a good approximation for large energy s, and the comparatively small s' associated with the low-energy resonances. The FESR and CMSR evaluations are done for amplitudes having good $s \longleftrightarrow u$ crossing properties; such amplitudes for photoproduction are the isoscalar photon amplitude $A^{(0)}$ and the isovector photon amplitudes $A^{(-)}$ and $A^{(+)}$ in terms of which the charged pion photoproduction amplitudes of (7) are given by

$$A_{i+} = (2)^{\frac{1}{2}}(A_i^{(0)} + A_i^{(-)})$$

$$A_{i-} = (2)^{\frac{1}{2}}(A_i^{(0)} - A_i^{(-)}) \qquad (i=1,2,3,4), \tag{11}$$

$A_i^{(0)}$, $A_i^{(+)}$, $A_j^{(-)}$ are crossing even and $A_j^{(0)}$, $A_j^{(+)}$, $A_i^{(-)}$ are crossing odd for $i = 1,2,4$ and $j = 3$. The calculations of Jackson and Quigg are for isovector (-) amplitudes (they use t-channel helicity amplitudes) so they are approximately proportional to the <u>difference</u> of the

$\gamma p \to \pi^+ n$ amplitudes (A_{i+}) and $\gamma n \to \pi^- p$ amplitudes (A_{i-}) calculated by our method of fixed-t dispersion relations.

From the crossing relations, as exhibited in Eqs. (7a), the high-energy amplitudes Re A_{i+} and Re A_{i-} calculated by fixed-t dispersion relations using the low-energy amplitudes are approximately equal and of opposite sign for $i = 1,2,4$; $A_{3\pm}$ are of the same sign but turn out to be smaller. Consequently, from (7), our calculated Re A are dominated by the isovector amplitudes Re $A^{(-)}$. We agree with Jackson and Quigg that the cross section of the forward spike is dominated by Re $A^{(-)}$ as calculated from low-energy amplitudes, and we have reinforced that conclusion by observing the convergent behavior of the amplitudes in that t region as a function of integration cutoff. But Jackson and Quigg also find agreement with some "average" of the $\gamma p \to \pi^+ n$ and $\gamma n \to \pi^- p$ cross sections over a much larger range of t. We would not attach any significance at all to this pseudo-model for $|t| \geq 0.2$ and we rather consider the rough agreement attained to be a fortuitous consequence of the particular integration cutoff which follows from our present state of knowledge of the low-energy amplitudes; to support this we pointed out in Sec. 2 above the behavior of the calculated real amplitudes as a function of integration cutoff in the region $-0.2 \geq t \geq -0.8$, which is qualitatively different from that in the spike region.

We point out one quite general feature associated with the decomposition (11) into isoscalar and isovector amplitudes of good crossing properties. At high energies $\frac{d\sigma}{dt}$ is proportional to $1/s^2$, while the polarized target experiments[18] reveal that there is both a real

and an imaginary part in important amplitudes. The simplest possibility to account for both these facts is that both the real and the imaginary part of the invariant amplitudes are proportional to $1/s$. If then the amplitudes are in a nonoscillatory asymptotic region and contain no logarithmic terms one can, as usual, apply the Phragmen-Lindeloff theorem to show that crossing even amplitudes are pure-imaginary and crossing-odd amplitudes pure real. From Eq. (11) and the crossing properties of the $A_i^{(0)}$ and $A_i^{(-)}$ it would then follow that $\frac{d\sigma}{dt}(\gamma p \to \pi^+ n) = \frac{d\sigma}{dt}(\gamma n \to \pi^- p)$ which is contrary to experiment. The conclusion is that we do not have a simple asymptotic regime of the type just outlined and in support we note that the polarization at 5 GeV/c is different from that at 16 GeV/c. It would be interesting to have results over a considerable range of high energy in various types of polarization experiment to elucidate the situation.

4. CHARGED PION PHOTOPRODUCTION BY POLARIZED PHOTONS

If $\sigma_\perp$ and $\sigma_{||}$ are the cross-sections for $\gamma N \to \pi N$ with photons polarized perpendicular and parallel to the production plane respectively, then at high energies $\sigma_\perp$ comes wholly from natural parity t-channel exchange and $\sigma_{||}$ from unnatural parity t-channel exchange. At 3 GeV/c the asymmetry ratio $A^\pm = \frac{\sigma_\perp - \sigma_{||}}{\sigma_\perp + \sigma_{||}}$ has been measured for $\pi^\pm$ photoproduction respectively. It is found that the asymmetry ratio A^+ for $\gamma p \to \pi^+ n$ is $A^+ \approx 0.7$ in the range $-0.2 > t > -0.8$ while the ratio A^- for $\gamma n \to \pi^- p$ is $A^- \approx 0.0$ in the same t range. Within the suggested quark model $A^+ = A^-$ (since the only difference in the model is in the charge of the proton quark and that of the neutron quark) giving an apparent disagreement between the data and the model. However, the cross-section for π^- production is small, so we would expect a large proportion of this amplitude to be outwith the model, for example from pion exchange which is unnatural parity and contributes to $\sigma_{||}$, thus reducing A. Indeed for $-0.2 > t > -0.8$ the charge ratio $\sigma_\perp(\gamma p \to \pi^- p)/\sigma_\perp(\gamma p \to \pi^+ n)$ is close to the exact model value of 25%, while the charge ratio for $\sigma_{||}$ is approximately unity. The inference is that the model contributes only to $\sigma_\perp$ (natural parity exchange) which dominates $\gamma p \to \pi^+ n$ and that the smaller $\sigma_{||}$ (unnatural parity exchange) only becomes important for $\gamma n \to \pi^- p$.

We show in Fig. 8 the ratio $A = (\sigma_\perp - \sigma_{||})/(\sigma_\perp + \sigma_{||})$ of the high-energy real parts as evaluated by the fixed-t dispersion relations from the low-energy resonances.

5. π^0 PHOTOPRODUCTION

In Fig. 9 we plot the contribution to the high-energy π^0 photoproduction cross section of the real parts of the amplitudes evaluated by the fixed-t dispersion relations. We show curves corresponding to the inclusion of successively higher mass resonances in the dispersion relations, as in the charged pion case. Unlike the charged pion case there is no uniform tendency; but like the charged pion case (for $-0.2 \geq t \geq -0.8$) there is no evidence of saturation of the dispersion relations by the low-energy resonances. When we bear in mind the uncertainties of the present data and the resulting partial wave analyses, it is probably not worthwhile to comment further on the confusing situation evident in Fig. 9.

There is no simple prediction on the ratio of neutral to charged pion photoproduction. However, if one considers the ratio

$$R_0 = \frac{d\sigma}{dt}(\gamma p \to \pi^0 p) \Big/ \frac{d\sigma}{dt}(\gamma n \to \pi^0 n) \tag{12}$$

it was shown in Ref. 19 by arguments based on our simple quark model of Fig. 2a that

$$\frac{4}{49} \leq R_0 \leq \frac{16}{25} \, . \tag{13}$$

It should be emphasized that the arguments leading to (13) involve the quark spins and thus (13) has not quite the same status as the charge ratios (5) and (6). The experiments have a result at or somewhat above the upper limit in (13), leading, as shown in Ref. 19, to quark-spin scalar dominance and strong dominance of $\sigma_\perp$ in neutral pion

photoproduction. Recent experimental results on the asymmetry $A = (\sigma_{\perp} - \sigma_{||})(\sigma_{\perp} + \sigma_{||})$ in π^0 photoproduction show that A is in the region of 0.9 to 1.0, corresponding to strong dominance of $\sigma_{\perp}$, except in the region of $t = -0.6$ where there is a drop in A to about $A = 0.8$. At $t = -0.6$ there is the well-known dip in π^0 photoproduction where presumably processes from outwith the model become relatively more important.

6. DISCUSSION AND CONCLUSIONS

We have noted in the introduction how the duality diagrams, combined with some weak vector meson dominance assumptions, lead to certain ratios for the imaginary parts of the amplitudes, Im A, for $\gamma N \to \pi^{\pm} N$ and $\gamma N \to \pi^{\pm}\Delta$; we have shown how the same ratios follow in an explicit quark model. Experimentally, and in the region $-0.2 \geq t \geq -0.8$, the predicted ratios on $|\mathrm{Im}\ A|^2$ hold for $\frac{d\sigma}{dt}$ which is proportional to $|\mathrm{Im}\ A|^2 + |\mathrm{Re}\ A|^2$; since the ratios are <u>not</u> predicted for Re A, because of the contribution to Re A of distant <u>u-channel</u> resonances, a problem is posed. The suggested resolution of the problem is that the combined contribution to Re A of the "low and medium energy" s- and u-channel resonances is negligible, so that Re A is either small compared to Im A or dominated by the "high-energy" s-channel resonances which would maintain the charge ratios in Re A. By explicit calculation, using fixed-t dispersion relations for $\gamma N \to \pi^{\pm} N$ it was shown that the cancellation of the contribution of low-energy s- and u-channel resonances to Re A, is strongly suggested by our present knowledge of the low-energy resonances (and the associated Im A from multipole analysis). On the other hand, in the region $0 > t > -0.2$, where the cross sections for $\gamma p \to \pi^{+} n$ and $\gamma n \to \pi^{-} p$ are tending towards equality in the forward direction the fixed-t dispersion relations are dominated by the very low-energy s- and u-channel resonances, in particular by the (gauge invariant) Born terms and the Δ, and $\left(\frac{d\sigma}{dt}\right)_{exp} \approx (\mathrm{Re}\ A)^2$, where Re A is found from the fixed-t dispersion relations.

The charge ratios for the imaginary part of the $\gamma N \to \pi^{\pm} N$ photoproduction amplitudes are given by

$$\mathrm{Im}\, A(\gamma n \to \pi^- p)/\mathrm{Im}\, A(\gamma p \to \pi^+ n) = \frac{1}{2}. \tag{14}$$

The duality diagram relations which, together with the assumption that a photon couples to vector mesons as a U-spin scalar, lead to (14) are[7]

$$\mathrm{Im}(\pi^- p \to \omega^0 n) = -\mathrm{Im}(\pi^- p \to \rho^0 n) \tag{15a}$$

$$\mathrm{Im}(\pi^+ n \to \omega^0 p) = -\mathrm{Im}(\pi^+ n \to \rho^0 p). \tag{15b}$$

Since the square of (14) holds experimentally for the cross sections, $(\propto |\mathrm{Re}\, A|^2 + |\mathrm{Re}\, A|^2)$ in the region $-0.2 > t > -0.8$ it is interesting to see whether the squares of (15) also hold experimentally for the cross sections $(\propto |\mathrm{Im}\, A|^2 + |\mathrm{Re}\, A|^2)$ in the same t region. We do have experimental information[20] both on $\pi^+ n \to \omega^0 p$ and $\pi^+ n \to \rho^0 p$ which suggests that, for $-0.2 > t > -0.8$

$$\frac{d\sigma}{dt}(\pi^+ n \to \omega^0 p) \simeq \frac{d\sigma}{dt}(\pi^+ n \to \rho^0 p)\ . \tag{16}$$

Another duality diagram predcition, related to $\gamma N \to \pi\Delta$, for which information exists on the corresponding cross section is

$$\mathrm{Im}(\pi^+ p \to \omega^0 \Delta^{++}) = \mathrm{Im}(\pi^+ p \to \rho^0 \Delta^{++}) \tag{17}$$

and experimentally,[21] for $-0.2 > t > -0.8$,

$$\frac{d\sigma}{dt}(\pi^+ p \to \omega^0 \Delta^{++})/\frac{d\sigma}{dt}(\pi^+ p \to \rho^0 \Delta^{++}) \simeq 1.5 \tag{18}$$

which is perhaps slightly worse agreement with the square of (17) than the photoproduction cross sections (2) are with (6). (We wish to remark the empirical status of our observations that the duality diagram relations hold good for the whole amplitude, in certain cases, and that concomitantly in $\pi^{\pm}$ photoproduction the contributions of the low-energy s- and u-channel resonances to the high-energy amplitude cancel. Since we have no theory we cannot foretell that such relations hold for all reactions. In particular similar whole amplitude duality diagram relations may very well not hold for kaon initiated reactions, since here the s and u channels have a dissimilar nature, one being exotic and one nonexotic.)

In the extreme forward direction $0 > t > -0.1$, for[20] $\pi^{+}n \rightarrow \rho^{0}p$, $\omega^{0}p$ and for[22] $\pi^{-}p \rightarrow \rho^{0}n$ the ρ^{0} cross section rises as $-t$ tends to zero and the ω^{0} cross section falls to zero, agreeing with the photoproduction through a vector meson dominance prescription.[23] Another way of stating this comparison, independently of any vector meson dominance assumption, is that the experiments on both $\gamma N \rightarrow \pi^{\pm}N$ and $\pi^{\pm}N \rightarrow \rho^{0}N$, $\pi^{\pm}N \rightarrow \omega^{0}N$ in the extreme forward direction $(0 > t > -0.1)$ are in some rough agreement with the Born approximation. It would be interesting to investigate in more detail the contribution of the Born approximation and other low-energy resonance (such as the lowest decuplet) to the real parts of the amplitudes for other non-elastic high-energy two-body reactions in the extreme forward direction.

If we were to take the naive quark model seriously we might have in mind the following picture of forward pion photoproduction. In the region of very small invariant four-momentum transfer, the (gauge

invariant) Born approximation amplitudes for $\gamma N \rightarrow \pi^{\pm} N$ represented by the diagrams of Fig. 3a for $\gamma N \rightarrow \pi^{\pm} N$ are important, maybe dominant, and give a forward spike. The amplitudes with Δ as intermediate state illustrated in Fig. 3b when added to the Born terms give a more pronounced forward spike, as shown in Fig. 7. This is compatible with a composite model in so far as for small momentum transfer the quark that is struck by the photon will tend to remain in the same spatial state, so that the intermediate state will tend to be that of the nucleon itself or the Δ which has the same spatial wave function as the nucleon in the quark model, as in the nucleon pole term of the Born approximation. When the struck quark is not excited the sum over intermediate states allows the pion to be emitted from a quark other than that which interacts with the photon (Fig. 3c); when such emissions from all possible quarks are taken into account we then regain the nucleon pole as an important part of the composite model. Strongly varying extreme forward behavior, also presumably associated with a guage invariant pion pole term, is observed for $\gamma N \rightarrow \pi^{\pm} \Delta$. At larger $-t$ than the extreme forward, or pion pole, region then spatial excitation of the quarks becomes more important and the photoproduction situation is as in Fig. 2a, leading to the charge ratios discussed above in the region $-0.2 \geq t \geq -0.8$. For $-0.8 > t$ one is in another region which would presumably correspond, in the quark model, to stronger interactions of the initially excited quark with the other quarks--that is, to multiple scattering.

FOOTNOTES AND REFERENCES

1. B. Richter, Proc. 1967 Stanford Electron-Photon Symposium, p. 309; H. Harari, Proc. 1967 Stanford Electron-Photon Symposium, p. 337; N. Dombey, Phys. Letters 30B, 646 (1969).
2. A. M. Boyarski, F. Bulos, W. Busza, R. Diebold, S. D. Ecklund, G. E. Fischer, J. R. Rees, and B. Richter, Phys. Rev. Letters 20, 300 (1968).
3. C. Geweniger, P. Heide, U. Kötz, R. A. Lewis, P. Schmüser, H. J. Skronn, H. Wahl, and K. Wegener, Phys. Letters 29B, 41 (1969); K. Lubelsmeyer, Proc. 1969 Daresbury Electron-Photon Conference, p. 45.
4. B. Richter, Proc. 14th International Conference on High Energy Physics, Vienna (1968); K. Lubelsmeyer, Proc. 1969 Daresbury Electron-Photon Conference, p. 45.
5. J. A. Campbell, R. B. Clark, and D. Horn, Phys. Rev. D2, 217 (1970).
6. G. L. Kane, F. Henyey, D. R. Richards, M. Ross, and G. Williamson, Phys. Rev.
7. The possibility of relations arising thus between the imaginary parts of photoproduction amplitudes was envisaged by H. Harari, Phys. Rev. Letters 22, 562 (1969).
8. See, for example, F. A. Berends, A. Donnachie, and D. L. Weaver, Nucl. Phys. B4, 3 (1967).
9. R. L. Walker, Phys. Rev. 182, 1729 (1969).
10. J. Engels, G. Schwiderski, and W. Schmidt, Phys. Rev. 166, 1343 (1968).

11. G. Buschhorn, P. Heide, U. Kötz, R. A. Lewis, P. Schmüser, and H. J. Skronn, Phys. Rev. Letters 20, 230 (1968).

12. R. G. Moorhouse and W. A. Rankin, Nucl. Phys. B23, 181 (1970).

13. In particular: (i) The large uncertainty for the $p_{11}(1470)$ pointed out in Ref. (12); (ii) As pointed out in Refs. (15) and (14) it is now believed that f_{15} photoproduction from neutrons is small, in contradiction to the Walker analysis.

14. R. L. Walker, Proc. 1969 Daresbury Electron-Photon Conference.

15. L. A. Copley, G. Karl, and E. Obryk, Nucl. Phys. B13, 303 (1969).

16. H. Harari, Annals of Phys. (to be published). (SLAC-PUB-821, 1970).

17. J. D. Jackson and C. Quigg, Phys. Letters 39B, 236 (1969); Nucl. Phys. B22, 301 (1970).

18. C. C. Morehouse et al., Phys. Rev. Letters 25, 835 (1970).

19. I. Barbour and R. G. Moorhouse, Nucl. Phys. B20, 629 (1970).

20. G. Bellettini, Proc. 14th International Conference on High Energy Physics, Vienna (1968); P. B. Johnson et al., Phys. Rev. 176, 1051 (1968).

21. G. S. Abrams et al., Phys. Rev. Letters 25, 617 (1970).

22. F. Bulos et al., SLAC-PUB-

23. C. F. Cho and J. J. Sakurai, Phys. Rev. D2, 517 (1970).

FIGURE CAPTIONS

Fig. 1. High energy differential cross sections for the processes $\gamma N \rightarrow \pi^{\pm}\Delta$.

Fig. 2. (a) Quark model diagram for pion photoproduction with s-channel excitation only. (b) Crossed diagram representing u-channel excitation only. (c) Duality diagram, equivalent to (a).

Fig. 3. (a) Feynman diagrams of Born approximation amplitudes for $\gamma N \rightarrow \pi^{\pm}N$; these amplitudes give a forward spike in the cross section. (b) Quasi-Born approximation amplitudes for $\gamma N \rightarrow \pi^{\pm}N$, with Δ instead of N as an intermediate state; these terms when combined with (a) give a more pronounced forward spike. (c) Schematic quark model diagram contributing to the Born or quasi-Born amplitudes.

Fig. 4. The s-plane cut structure used in the fixed-t dispersion relations. The physical s-value corresponding to incoming photon momentum of 16 GeV/c is shown, and the diagram illustrates that the dispersion relation energy denominators $1/(s'-s)$ vary little as s' ranges over the low-energy cut region where the amplitudes are known. (The cut structure is shown for $t = 0$; as $-t$ increases the left- and right-hand cuts move towards each other and eventually overlap.)

Fig. 5. The contribution to $(s - M^2)^2\, d\sigma/dt$ arising from the real parts of the high-energy charged pion photoproduction amplitudes as evaluated using the fixed-dispersion relations (7). The various curves represent the results as singularities and resonances

for successively higher s' are included in $\mathrm{Im}\, A(s',t)$. The lowest curve is the result when all the resonances in the solid (Fig. 4) region are included plus the $f_{37}(1920)$ which is just outside the solid region; and the dots show the result when the non-resonant background within the solid region is also included. The curves shown are for $\gamma p \to \pi^+ n$, but the $\gamma n \to \pi^- p$ curves are almost indistinguishable. The curves, and the experimental points showing the $\pi^+ n$ and $\pi^- p$ data, are also nearly independent of s, for s large.

Fig. 6. The contribution to $(s - M^2)^2 \; d\sigma/dt$ of the real part of the high-energy amplitudes at a fixed value of $t = -0.4$, as evaluated from the dispersion relations (7). The abscissa s' represents the cut-off in the upper limit of integration in (7), and the plotted line is the result of using (7) with upper limit of integration s'. (This graph can be obtained from the values given in Fig. 5 for $t = -0.4$.)

Fig. 7. The contribution of $(s - M^2)^2 \; d\sigma/dt$ of the real part of the high-energy amplitudes evaluated from the fixed-t dispersion relations, plotted as a function of $(-t)^{1/2}$ in the forward spike region. The experimental points are for $\gamma p \to \pi^+ n$ at various energies.[2]

Fig. 8. The curve shows the high energy $\gamma p \to \pi^+ n$ or $\gamma n \to \pi^- p$ asymmetry ratio $A = (\sigma_\perp - \sigma_{||})/(\sigma_\perp + \sigma_{||})$ for polarized photons, where $\sigma_\perp$ and $\sigma_{||}$ are the contributions to the cross sections from the real parts evaluated using the fixed-t

dispersion relations, integrated over the low-energy resonances. Some representative experimental points[3] are shown as ⧗ for $\gamma p \rightarrow \pi^+ n$ and ⧗ for $\gamma n \rightarrow \pi^- p$.

Fig. 9. The contribution to $(s - M^2)^2\, d\sigma/dt$ arising from the real parts of the high-energy $\gamma p \rightarrow \pi^0 p$ photoproduction amplitudes as evaluated using the fixed-t dispersion relations (7) at 16 GeV/c. The different curves show the inclusion of successively higher mass resonances in (7) and the crosses are a representation of the experimental high-energy data. Curves 1, 2, 3, and 4 include resonances through, respectively, $s_{11}(1560)$, $d_{13}(1520)$, $f_{15}(1690)$, $f_{37}(1920)$. Curve 5 includes resonances plus non-resonant background.

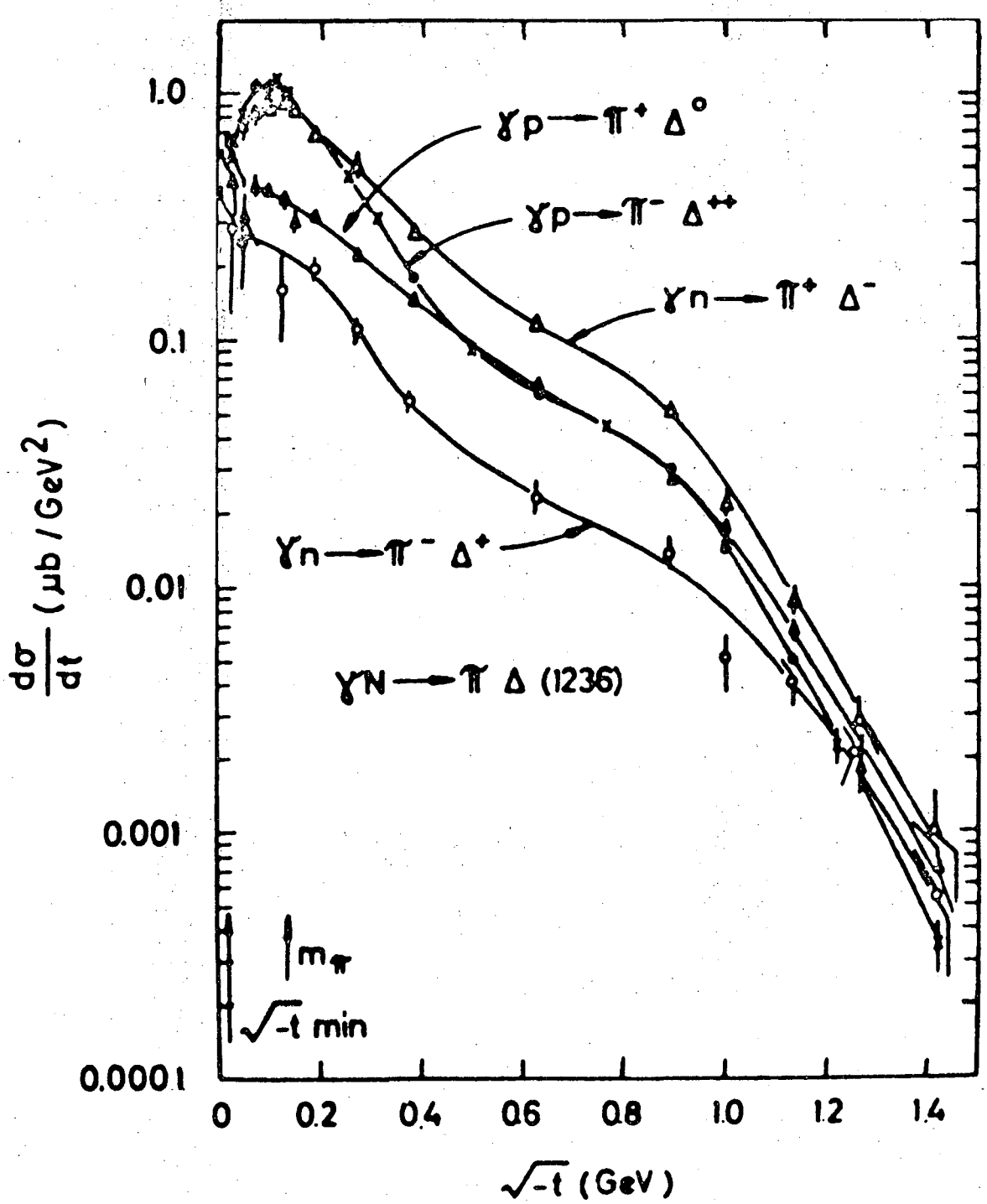

XBL 713-533

Fig. 1.

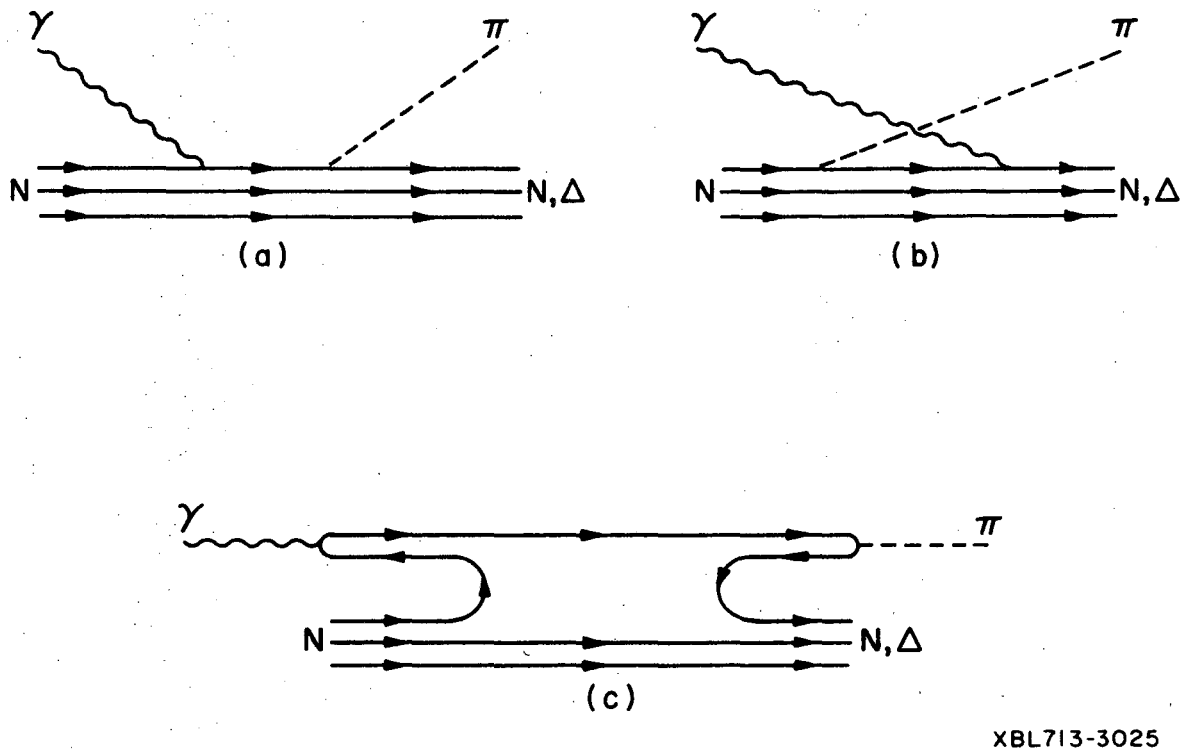

Fig. 2.

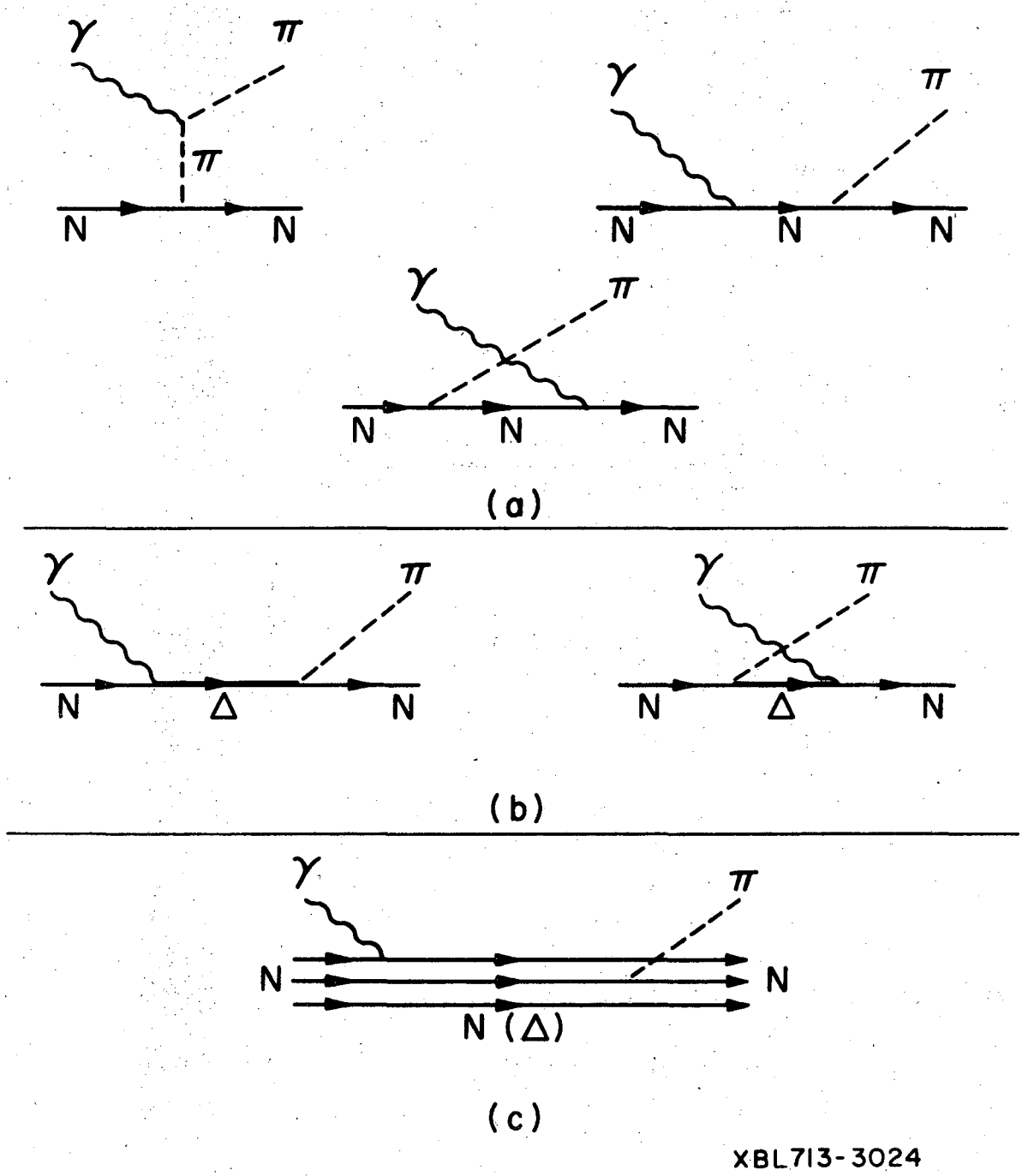

Fig. 3.

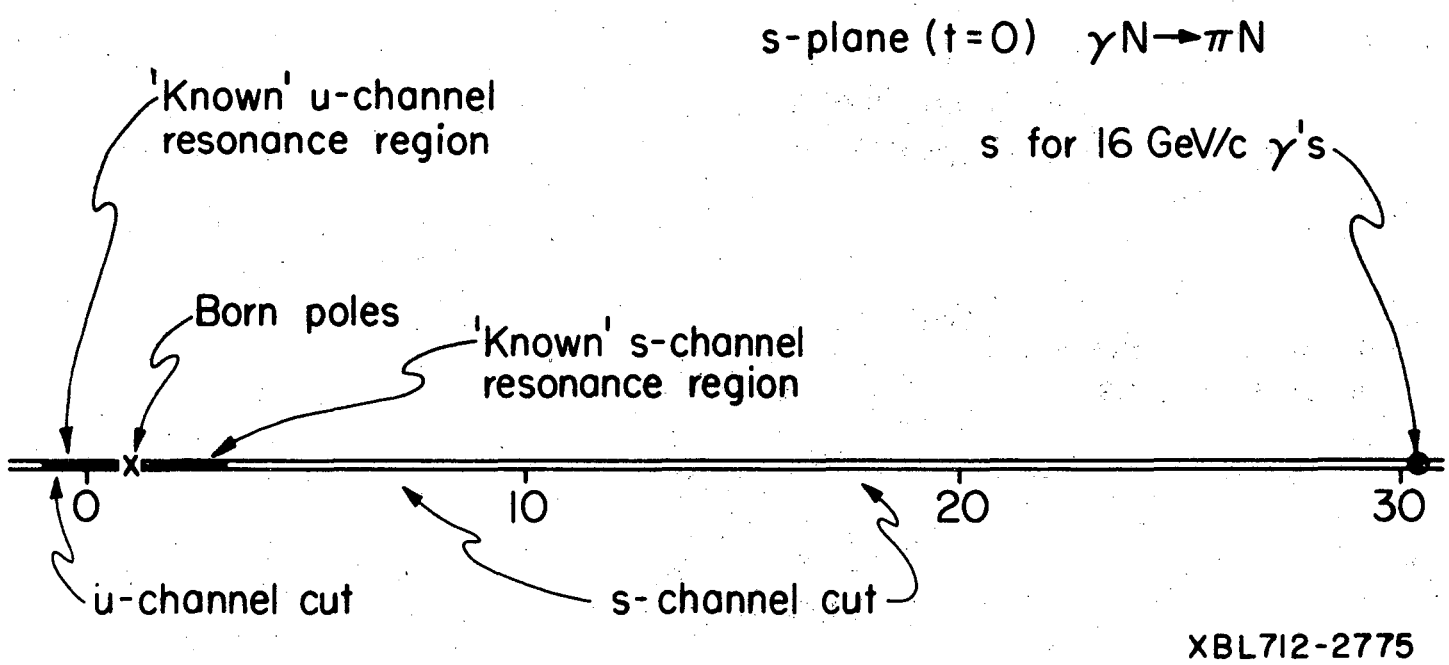
s-plane (t=0) γN→πN
'Known' u-channel resonance region
s for 16 GeV/c γ's
Born poles
'Known' s-channel resonance region
0
10
20
30
u-channel cut
s-channel cut
XBL712-2775

Fig. 4.

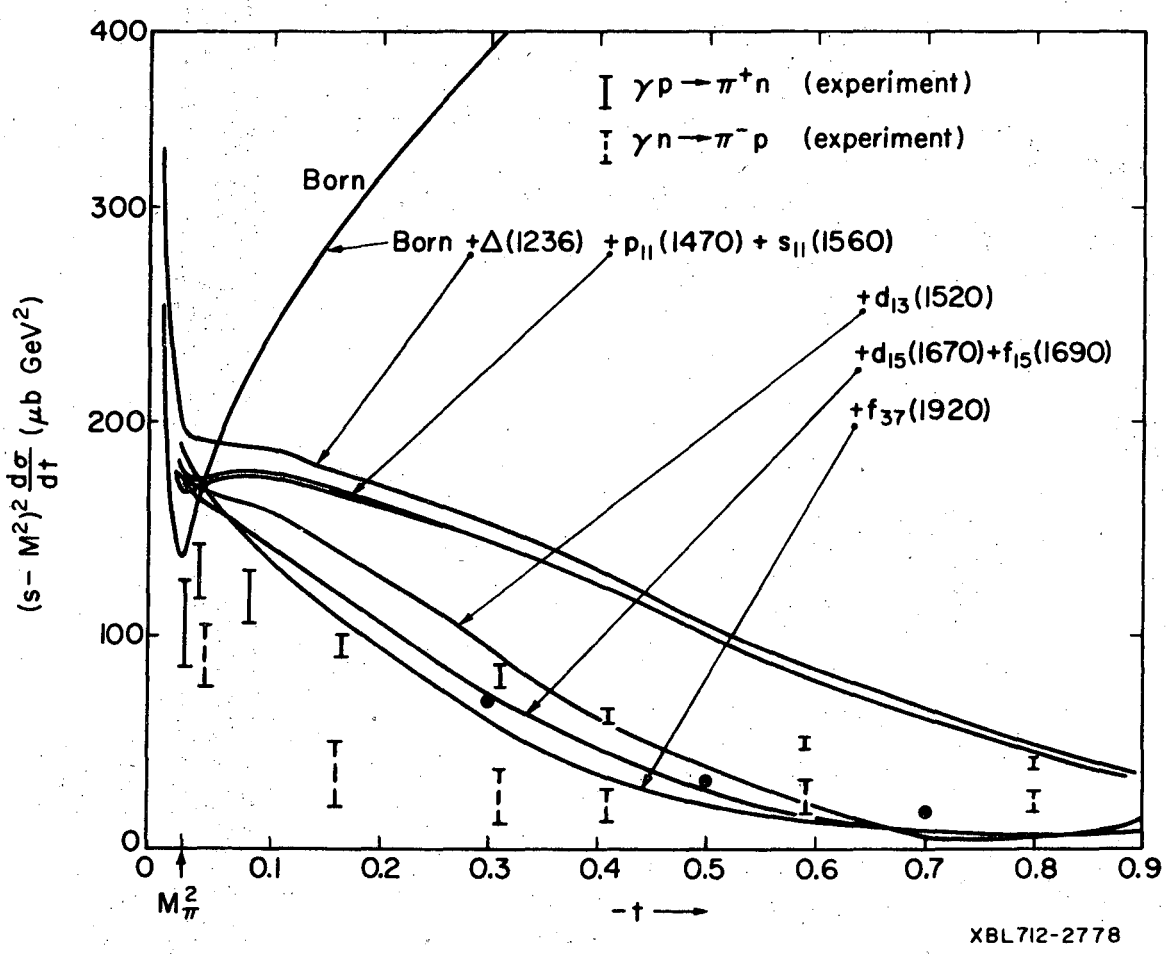
400
300
200
100
0
0
0.1
0.2
0.3
0.4
0.5
0.6
0.7
0.8
0.9
M_π^2
$-t$
$(s-M^2)^2 \frac{d\sigma}{dt}$ (μb GeV^2)
$\gamma p \to \pi^+ n$ (experiment)
$\gamma n \to \pi^- p$ (experiment)
Born
Born +Δ(1236) +p_{11}(1470) + s_{11}(1560)
+d_{13}(1520)
+d_{15}(1670)+f_{15}(1690)
+f_{37}(1920)
XBL712-2778

Fig. 5.

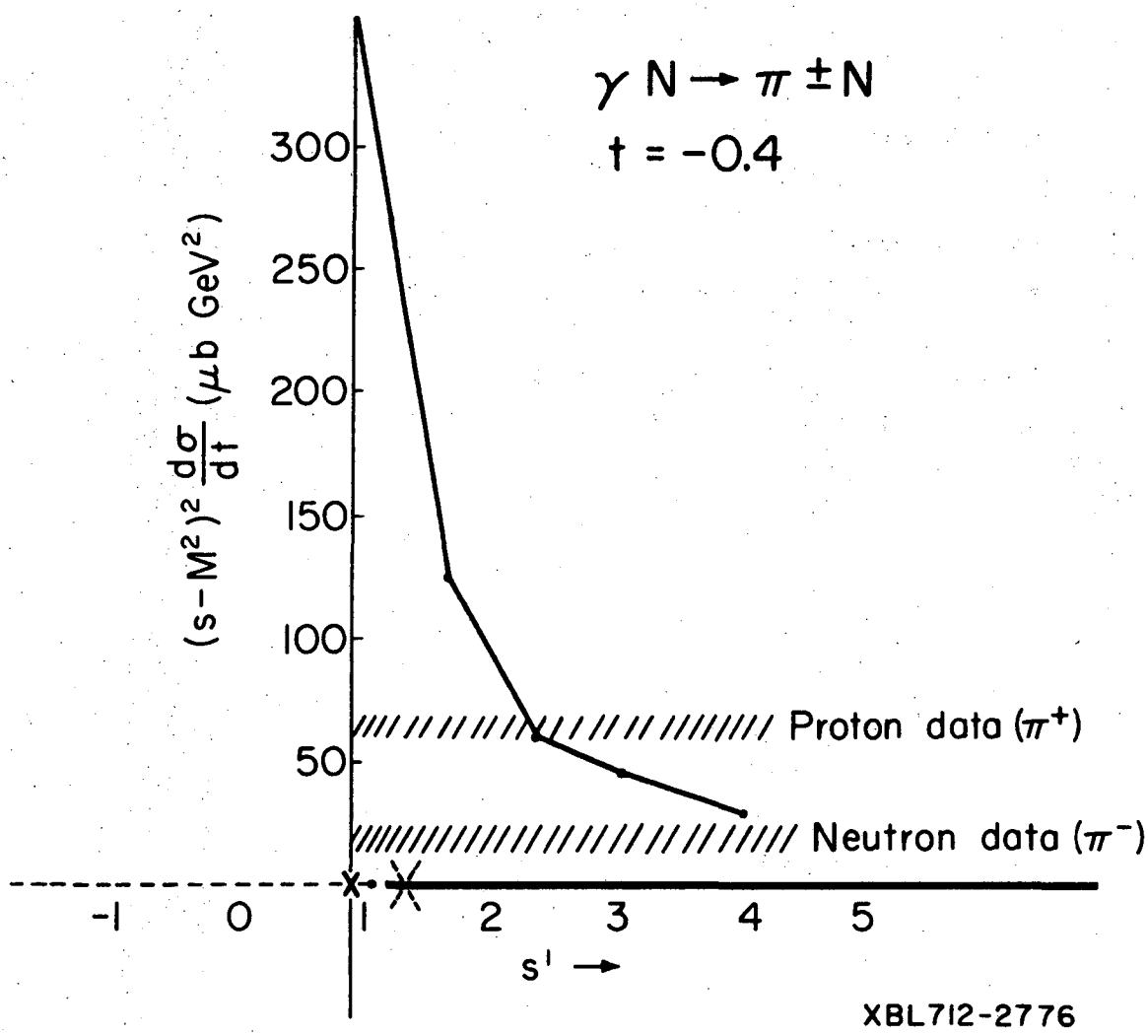
γ N → π ± N
t = −0.4
300
250
200
150
100
50
(s−M²)² dσ/dt (μb GeV²)
Proton data (π⁺)
Neutron data (π⁻)
-1
0
1
2
3
4
5
s' →
XBL712-2776

Fig. 6.

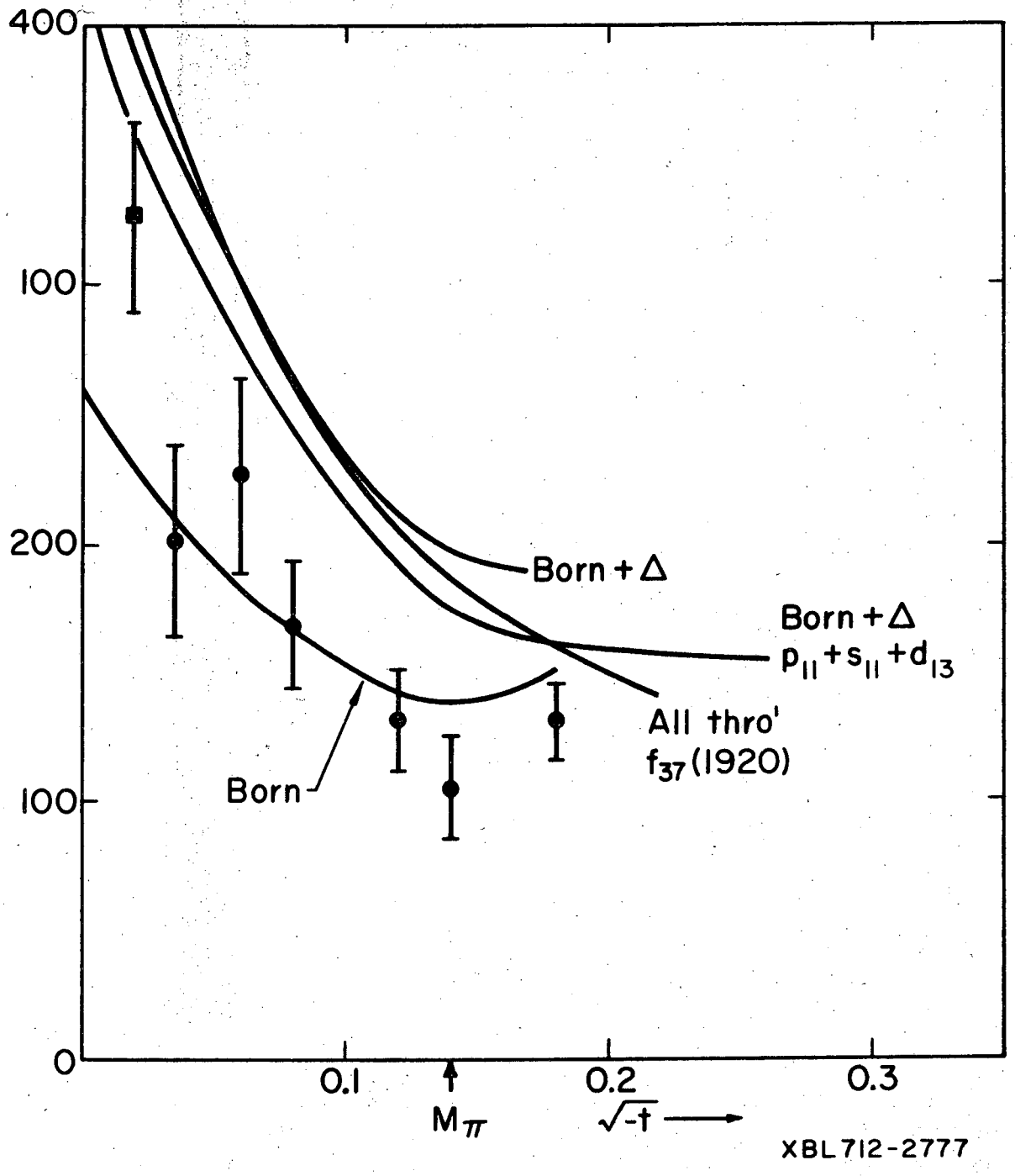
400
100
200
100
0
0.1
0.2
0.3
M_π
$\sqrt{-t}$
Born + Δ
Born + Δ
$p_{11} + s_{11} + d_{13}$
All thro'
$f_{37}(1920)$
Born
XBL712-2777

Fig. 7.

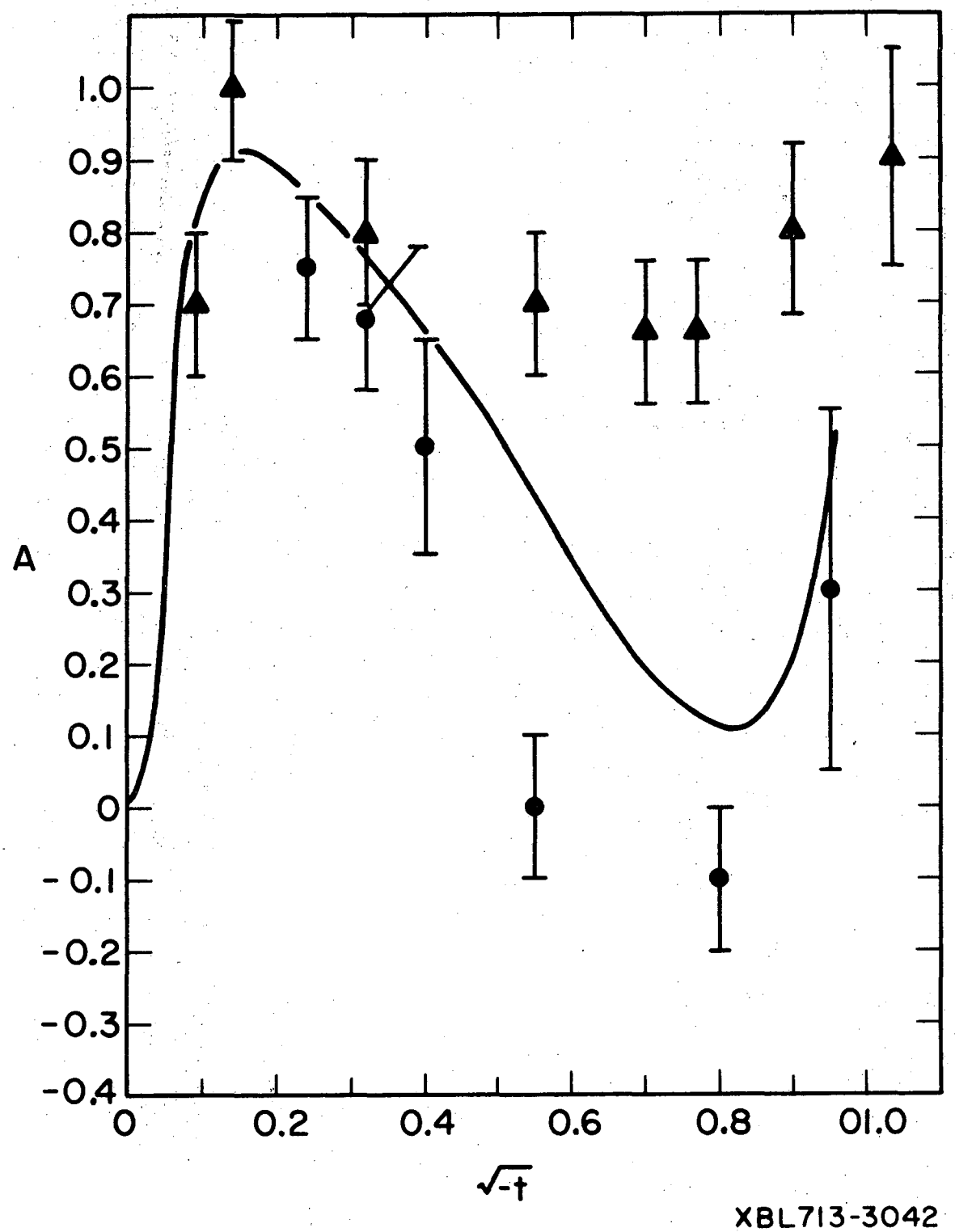
1.0
0.9
0.8
0.7
0.6
0.5
0.4
A
0.3
0.2
0.1
0
-0.1
-0.2
-0.3
-0.4
0
0.2
0.4
0.6
0.8
01.0
√-t
XBL713-3042

Fig. 8.

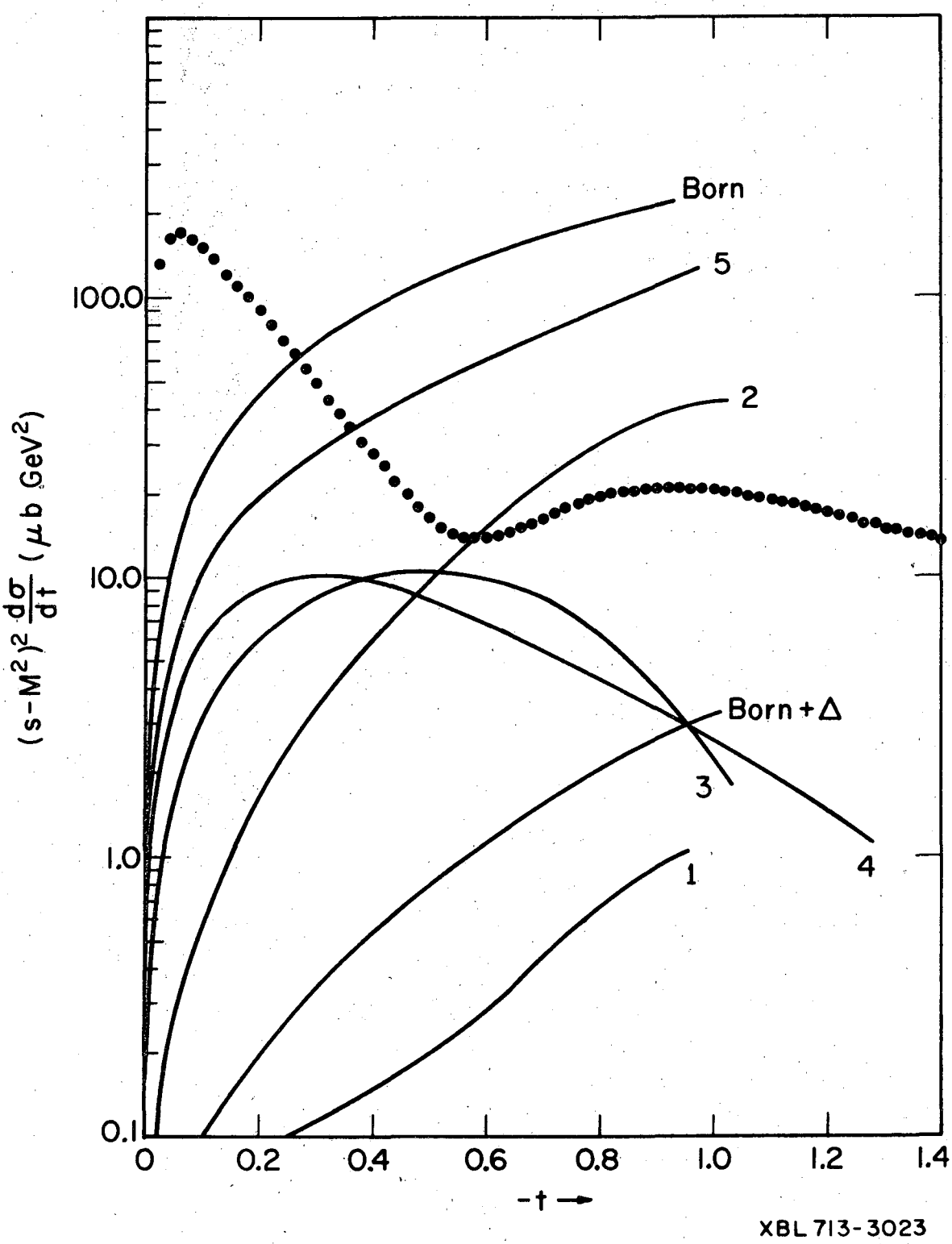
Born
5
2
Born + Δ
3
4
1
100.0
10.0
1.0
0.1
0
0.2
0.4
0.6
0.8
1.0
1.2
1.4
-t →
$(s-M^2)^2 \frac{d\sigma}{dt}$ (μb GeV^2)
XBL 713-3023

Fig. 9.

LEGAL NOTICE

This report was prepared as an account of work sponsored by the United States Government. Neither the United States nor the United States Atomic Energy Commission, nor any of their employees, nor any of their contractors, subcontractors, or their employees, makes any warranty, express or implied, or assumes any legal liability or responsibility for the accuracy, completeness or usefulness of any information, apparatus, product or process disclosed, or represents that its use would not infringe privately owned rights.

TECHNICAL INFORMATION DIVISION
LAWRENCE RADIATION LABORATORY
UNIVERSITY OF CALIFORNIA
BERKELEY, CALIFORNIA 94720